International Journal on Recent and Innovation Trends in Computing and Communication
ISSN: 2321-8169 Volume: 11 Issue: 10s
DOI: https://doi.org/10.17762/ijritcc.v11i10s.7703
***Article Received:** 12 June 2023 **Revised:** 30 July 2023 **Accepted:** 10 August 2023*

Automated Identification and Localization of Brain Tumor in MRI Using U-Net Segmentation and CNN-LSTM Classification

Chandrakantha T S[1], Basavaraj N Jagadale[2], Abhisheka T E[3], Omar Abdullah Murshed Farhan Alnaggar[4]
[1]Research Scholar
Department of PG Studies and Research in Electronics
Kuvempu University, Shimoga,India
chandrabeluved@gmail.com
[2]Associate Professor
Department of PG Studies and Research in Electronics
Kuvempu University, Shimoga,India
basujagadale@gmail.com
[3]Research Scholar
Department of PG Studies and Research in Electronics
Kuvempu University, Shimoga,India
te.abhishek@gmail.com
[4]Research Scholar
Department of PG Studies and Research in Electronics
Kuvempu University, Shimoga,India
alnaggar1994@gmail.com

Abstract— Nowadays, the use of computers to evaluate medical images automatically is critical part of the life. Today's treatment method relies heavily on early diagnosis and accurate disease identification, which were formerly difficult for medical research to achieve. Brain Magnetic Resonance Imaging (MRI) is essential to the detection and treatment of brain tumor (BT). Tumor of the brain are the result of brain cell division that has gone awry or is otherwise out of control. The manual MRI segmentation of BT is a difficult and time-consuming process. The most critical factor in the effective treatment and identification of BT is the ability to accurately locate the tumor. The detection of BT is regarded as a difficult task in medical image processing. For analysing and interpreting MRI, there are semi-automatic and fully automated systems that require large-scale professional input and evaluation, with varying degrees of effectiveness. Automated identification and extraction of the tumor's localization from brain MRI will be proposed in this paper. To achieve this goal, the data collected from Kaggle and the collected data are processed. Then the U-Net is employed to segment the tumor region from the MRI. Next, the MRI is classified using DL models like Convolutional Neural Network (CNN), and the hybrid Convolutional Neural Network and Long Short-Term Memory (CNN-LSTM). Both process segmentation and classification are evaluated using the metrics. From the evaluation, it is identified that CNN-LSTM outperforms the CNN model.

Keywords- Brain, Tumor, Augmentation, Resize, Segmentation, Accuracy, Loss.

I. INTRODUCTION

The detection and classification of organ abnormalities, including leukemia, colon cancer, brain tumor, breast cancer, bowel cancer, skin cancer, and optic image analysis, are crucial aspects of medical imaging classification. Organ defects and tumor growth are closely linked and can lead to fatalities [1]. Brain tumors (BT) are particularly serious as they affect the central nervous system and can occur in both children and adults. BTs can be benign or malignant, with malignant tumors being highly dangerous and requiring accurate diagnosis for effective treatment [2].

Medical imaging, especially MRI, heavily relies on computer technology, and image segmentation plays a fundamental role in medical image analysis [3]. Various segmentation methods are used to accurately categorize tumors from MRI images, improving classification success rates [4]. Ensembling features and using Convolutional Neural Networks (CNN) are effective techniques for tumor segmentation and classification [5][6][7]. Other approaches combine clustering methods with CNN for efficient segmentation [8][9]. Transfer learning is also employed to enhance classification performance [10].

International Journal on Recent and Innovation Trends in Computing and Communication
ISSN: 2321-8169 Volume: 11 Issue: 10s
DOI: https://doi.org/10.17762/ijritcc.v11i10s.7703
***Article Received:** 12 June 2023 **Revised:** 30 July 2023 **Accepted:** 10 August 2023*

A deep learning-based multiscale approach for brain tumor segmentation and classification demonstrates the advantage of processing input images at different spatial scales via different processing routes [7]. The use of Shuffled Frog-Leaping Algorithm (SFLA) for CNN optimization shows improved classification accuracy [13]. Additionally, combining semantic segmentation with CNN helps accurately predict the presence of a tumor in MRI images [11]. A hybrid model that combines U-Net segmentation and CNN-LSTM classification is proposed to enhance the accuracy of BT detection [12].

Although significant progress has been made in BT detection, there is still room for improvement. Future research can focus on further enhancing the accuracy and efficiency of tumor segmentation and classification. The proposed hybrid model of U-Net segmentation and CNN-LSTM classification can be explored to automate the BT detection process effectively [15].

II. METHODOLOGY

The methodology involved in the segmentation and classification of the BT is detailed in this chapter. The steps involved are detailed below:

- Data collection: The BT and non-tumor MRI images and its mask are collected from the Kaggle website.
- Data processing: The collected raw MRI is processed using techniques like resizing, normalizing, and augmentation.
- Segmentation: The tumor region is segmented from the MRI using the U-Net model. And the constructed U-Net model is evaluated using the metrics IoU and Dice coefficient.
- Classification: The MRI is classified using a DL model like CNN and CNN-LSTM. The model is trained and validated using 80% and 10% of the whole data. Finally, the model is tested using the remaining10% data. Each model is evaluated using metrics of accuracy and loss.

The methodology is represented in the flow chart as shown in figure 1.

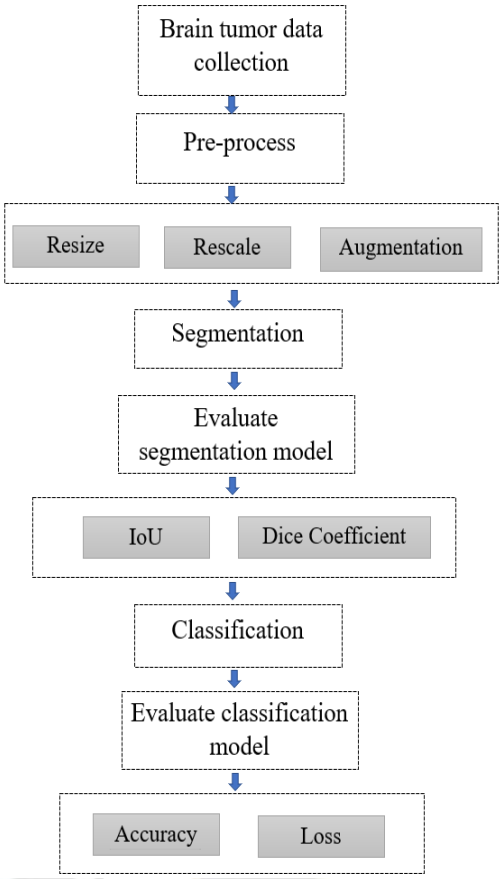

Figure 1. BT segmentation and classification process flow

III. DATA COLLECTION AND PROCESS

The dataset was obtained from Kaggle [Kaggle website], and it consists of brain MR images with custom fluid-attenuated inversion recovery (FLAIR) aberrant segmentation masks. The images were obtained from The Cancer Imaging Archive (TCIA). These belong to 110 individuals from The Cancer Genome Atlas (TCGA) lower-grade glioma sample with whom sequencing and genomic cluster data are available. Figure 2 shows the gathered BT data and it is composed of MRI, mask, and label. Mask is used for identifying the tumor region and a label is used to identify whether the tumor is present or not.

	image	mask	label
0	kaggle_3m\TCGA_CS_4941_19960909\TCGA_CS_4941_1...	kaggle_3m\TCGA_CS_4941_19960909\TCGA_CS_4941_1...	0
1	kaggle_3m\TCGA_CS_4941_19960909\TCGA_CS_4941_1...	kaggle_3m\TCGA_CS_4941_19960909\TCGA_CS_4941_1...	1
2	kaggle_3m\TCGA_CS_4941_19960909\TCGA_CS_4941_1...	kaggle_3m\TCGA_CS_4941_19960909\TCGA_CS_4941_1...	1
3	kaggle_3m\TCGA_CS_4941_19960909\TCGA_CS_4941_1...	kaggle_3m\TCGA_CS_4941_19960909\TCGA_CS_4941_1...	1
4	kaggle_3m\TCGA_CS_4941_19960909\TCGA_CS_4941_1...	kaggle_3m\TCGA_CS_4941_19960909\TCGA_CS_4941_1...	1

Figure 2. BT data

The collected MRI and its corresponding mask are shown in figure 3. The figure consists of four rows, the first row contains a tumor image and the second contains a tumor mask image, similarly the third and fourth are composed of non-tumor MRI and its mask image.

International Journal on Recent and Innovation Trends in Computing and Communication
ISSN: 2321-8169 Volume: 11 Issue: 10s
DOI: https://doi.org/10.17762/ijritcc.v11i10s.7703
***Article Received:** 12 June 2023 **Revised:** 30 July 2023 **Accepted:** 10 August 2023*

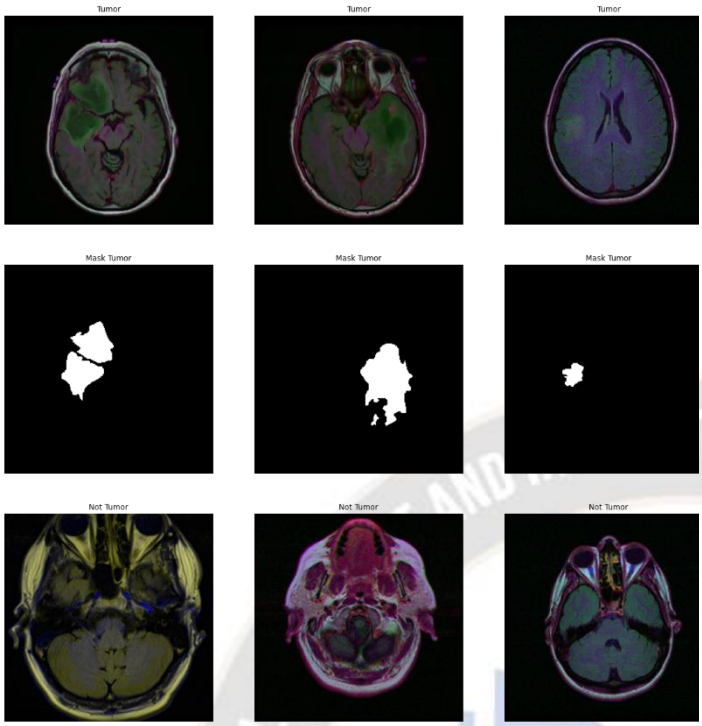

Figure 3. Brain MRI image and its tumor mask

The collected raw images undergo essential pre-processing steps, including resizing, normalization, and augmentation, to make them suitable for segmentation and classification tasks. Resizing images is a crucial step in computer vision, as deep learning algorithms generally perform better when trained on smaller images [16]. Smaller input images reduce the number of computations, leading to shorter training times for neural models.

Data normalization ensures that input parameters have a uniform distribution, as it transforms floating-point attribute values to a new range, typically between 0 and 1. This process helps create a Gaussian distribution of pixel values, making data uniformly dispersed within the defined range [17]. The widely used min-max standardization technique is employed to normalize the pixel values in this study [17].

Data augmentation is a powerful technique that enhances the diversity of the dataset by generating new images with slight variations. This process is akin to imagination or daydreaming, where diverse scenarios are envisioned to gain a better understanding of the subject matter[18]. Data augmentation methods simulate changes such as rotation, shift, shear, zoom, and flip in the images, thereby increasing the robustness of the model [19].

IV. SEGMENTATION

Even though there are many DL images available, U-Net was created exclusively for biomedical image segmentation. The U-Net architecture has proven to be particularly effective for biomedical image segmentation. In comparison to earlier models, this one requires only a minimum of annotated images and execution time. The main segmentation stage was carried out with the help of a full CNN and the U-Net. As a result, U-Net Model was selected for the KiTS competition 2019. In contrast to typical CNN models, the U-Net model works well with smaller datasets. Because labelled training data is scarce in medical imaging, the U-Net design is based on a modified version of the Fully Convolutional Network [20]and the U-Net is based on two distinct principles:

• The U-design net is perfectly symmetrical.

• Skip connections between the up and downsample paths use a concatenation administrator rather than an entirely.

Skip associations imply that local data is given preference over global data when upsampling. Due to its symmetry, the networks' upsampling approach includes a high amount of feature maps, that facilitate information exchange. Because of the upsampling strategy, the initial design featured a significant number of classes in feature maps[21]. The U-Net design is depicted in Figure 4.

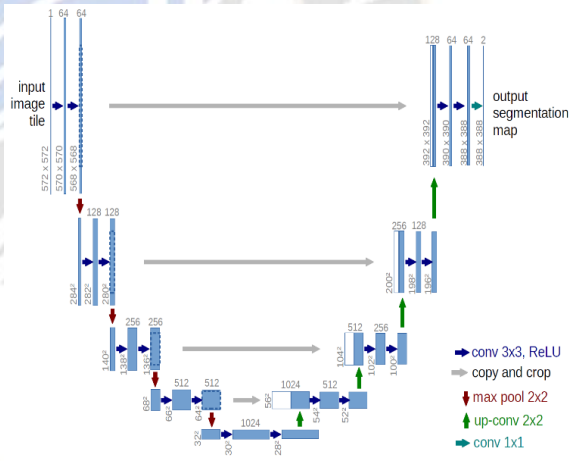

Figure 4. U-Net Architecture[24]

U-Net is made of contracting path (left) and an enlarged path (right). The convolutional (Conv) layers are stacked one on top of the other on the contracting route, with max-pool as the final layer. It starts with two unpadded 3x3 convolutions, and a 2x2 pooling with a stride rate of two. An autoencoder encodes input data into a different representation and decodes the output back into the original format. This video shows a representation learning algorithm in operation. An auto-encoder is programmed to retain as much information as possible by passing it through the encoder and decoder many times before usage. To create the new representation, auto-encoders are also taught. With each downsampling step, a 2x2 Conv ("up-convolution") splits the extracted features in half,

International Journal on Recent and Innovation Trends in Computing and Communication
ISSN: 2321-8169 Volume: 11 Issue: 10s
DOI: https://doi.org/10.17762/ijritcc.v11i10s.7703
***Article Received:** 12 June 2023 **Revised:** 30 July 2023 **Accepted:** 10 August 2023*

concatenated with the suitably separated extracted features from the contracting path, and two 3x3 Conv, usually accompanied by a ReLU, raise the number of highlight channels. Because pixels are lost on the edges during every Conv, the image needs to be cropped. At the last layer, a 1x1 Conv is employed to move the 64-feature descriptor to the number of categories that were chosen earlier. The system has a total of 23 Conv layers. The conv2d block, which employs Conv layers, follows normalization and the ReLU function in the U-net model.

V. CLASSIFICATION

For BT classification DL technology is used. In DL, CNN and CNN-LSTM are chosen to predict the tumor from MRI. The architecture and working of both algorithms are detailed in this section.

A. CNN (Convolutional Neural Network)

CNNs are powerful neural networks that excel in pattern recognition and image processing tasks [25][26]. They consist of a large number of layers and are specifically designed for extracting local features from input data and gradually transforming them into more sophisticated features. CNNs use convolutional, pooling, and fully connected layers. The convolutional layer employs a set of kernels to produce feature mappings, and the pooling layer downsamples the input to reduce the number of parameters, often using max pooling [28]. The fully connected layer serves as a classifier to make predictions based on the extracted features [27].

B. CNN-LSTM (Convolutional Neural Network - Long Short-Term Memory)

CNN-LSTM is an enhancement of the recurrent neural network (RNN) architecture known as Long Short-Term Memory (LSTM). LSTM overcomes issues of vanishing and exploding gradients encountered in traditional RNNs by incorporating memory blocks and a cell state to retain long-term information [28]. LSTM networks typically consist of input, forget, and output gates. The input gate decides which part of the input and previous output to include using a sigmoid layer. The forget gate selectively determines what information to discard from the previous cell state using a sigmoid layer and dot product. The output gate calculates the states necessary for generating the final output based on new data from the state decision vectors [29].

The proposed hybrid framework combines the strengths of both CNN and LSTM by using CNN for feature extraction and LSTM for categorization. This integration allows the model to extract relevant features from the input data using CNN and then utilize LSTM to make sequential predictions based on the extracted features [30].

VI. RESULTS AND DISCUSSION

The BT data was collected from the Kaggle website. The data contain both tumor and non-tumor images with masks. The image is first processed to make the image ready to give as input to the segmentation and classification model. The process such as resizing, normalization, and augmentation is done. Next processing segmentation and classification task are deployed on the images. For segmentation, U-Net is used and for classification CNN and CNN-LSTM models are utilized. In this research the CNN-LSTM is the suggested approach to classify the tumor and its effectiveness is described by comparing the results with conventional CNN. In CNN, both feature extraction and classification are done in same network. But in CNN-LSTM, the feature extraction is done by CNN and classification by done by LSTM. It takes the advantages of both CNN and LSTM model.

A. Segmentation

The U-Net is employed to segment the tumor region from MRI. First, the U-Net is trained using 80% of collected data and validated by 10% of data. For analysis, the IoU and Dice coefficients metrics are used. The number of epochs used to train the model is 50. At each epoch, the IoU and Dice coefficient obtained by train and validation phase is plotted in Figures 5 and 6. The green and orange plot in Figure 5 is used to represent the IoU values of the validation and training phase under epochs. The black and blue plot in Figure 6 is used to represent the Dice values of validation and training phase under epochs.

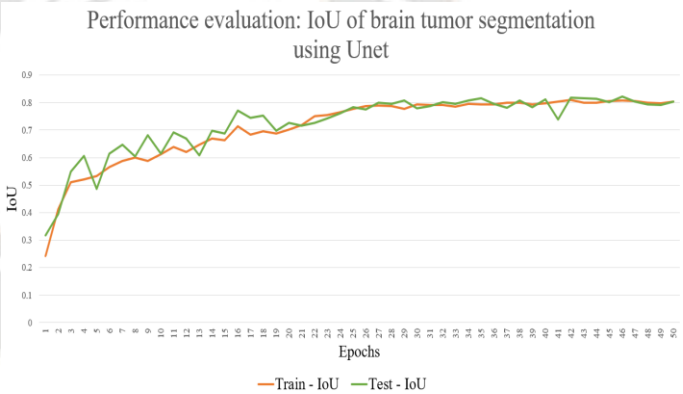

Figure 5. U-Net IoU plot on BT segmentation Net

International Journal on Recent and Innovation Trends in Computing and Communication
ISSN: 2321-8169 Volume: 11 Issue: 10s
DOI: https://doi.org/10.17762/ijritcc.v11i10s.7703
***Article Received:** 12 June 2023 **Revised:** 30 July 2023 **Accepted:** 10 August 2023*

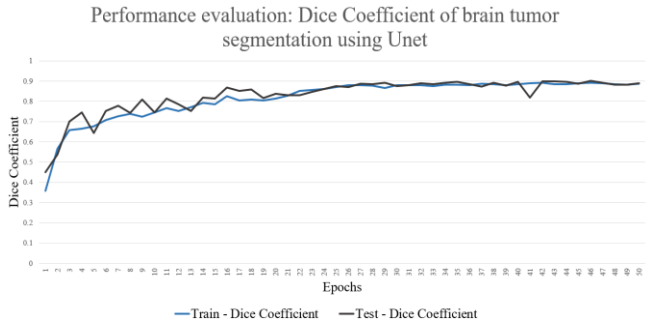

Figure 6. U-Net Dice coefficient plot on BT segmentation

Table 1 shows the result of the U-Net system on the segmentation of tumors using test data. The IoU and Dice Coefficient values are 0.79445 and 0.8843. The attained values are nearer to 0.80 and it shows that the segmented model designed is good enough for identifying tumor regions. Figure 7 shows the segmentation of tumors using U-Net. The figure consists of three images, the 1st demonstrates the raw MRI, the 2nd illustrates the original mask, and the 3rd displays the predicted tumor. The first row is the result of the tumor image and the second row shows the result of the non-tumor image.

TABLE I. U-Net segmentation result on test data

Metrics	**Test IOU**	**Test Dice Coefficient**
Formula	$IOU = \frac{TP}{TP + FP + FN}$	$DICE = \frac{2 * TP}{(TP + FP) + (TP + FN)}$
Metrics value	0.79445	0.8843
Where, TP and TN → True Positive and Negative, FP and FN → False Positive and Negative		

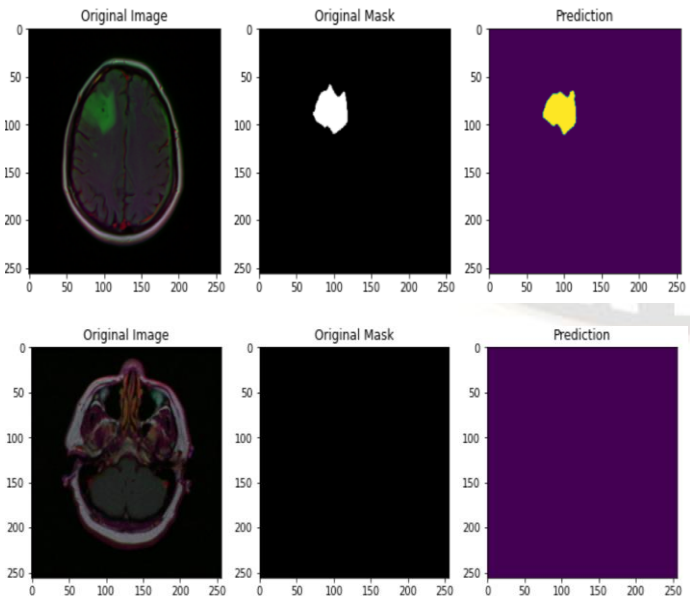

Figure 7. U-Net BT segmentation

B. *Classification*

For classification two models are employed such as CNN and CNN-LSTM. To evaluate the model the metrics like accuracy and loss are chosen. Both models are divided into three stages, such as train, validate and test. The accuracy attained by CNN in the train and validate phase is shown in Figure 8. The two different colors red and black are used to show the difference in training and validation results. Similarly, in the train and validate phases, CNN's loss value is presented in Figure 9. The difference between training and validation results is shown by the use of two different colors, such as red and blue.

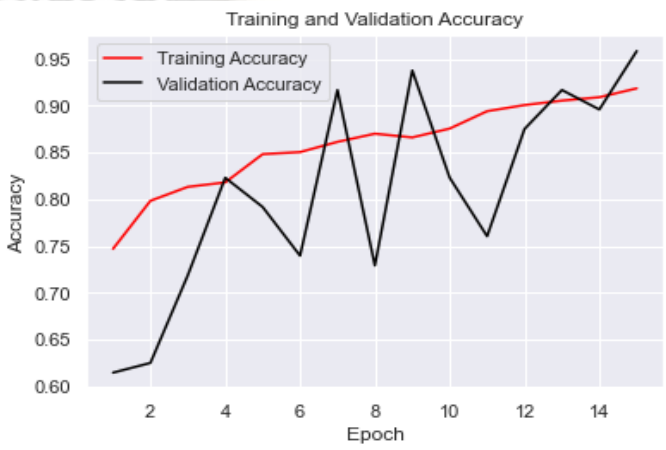

Figure 8. CNN Accuracy on BT classification

Figure 9. CNN Loss on BT classification

The test images are given to the CNN model to predict whether the image contains a tumor or not. The accuracy and loss attained in the testing phase are 0.9033 and 0.2423 and the result is depicted in Figure 10. The figure clears that the time taken to predict the test images is 411ms.

```
25/25 [==============================] - 10s 411ms/step -
loss: 0.2423 - accuracy: 0.9033
```

Figure 10. CNN outcome on test data

International Journal on Recent and Innovation Trends in Computing and Communication
ISSN: 2321-8169 Volume: 11 Issue: 10s
DOI: https://doi.org/10.17762/ijritcc.v11i10s.7703
***Article Received:** 12 June 2023 **Revised:** 30 July 2023 **Accepted:** 10 August 2023*

Figure 11 depicts the accuracy reached by CNN-LSTM during the train and validate phases. Green and blue are two different colors used to highlight the difference between training and validation results. Figure 12 shows the CNN-LSTM loss value during the train and validate phases. The use of two different colors, such as red and green, shows the difference between training and validation outcomes.

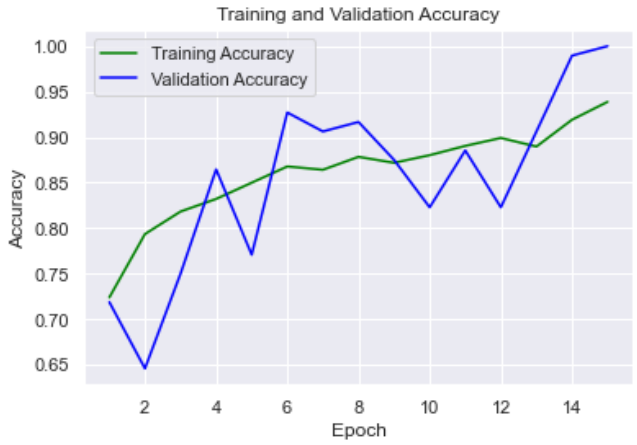

Figure 11. CNN-LSTM Accuracy on BT classification

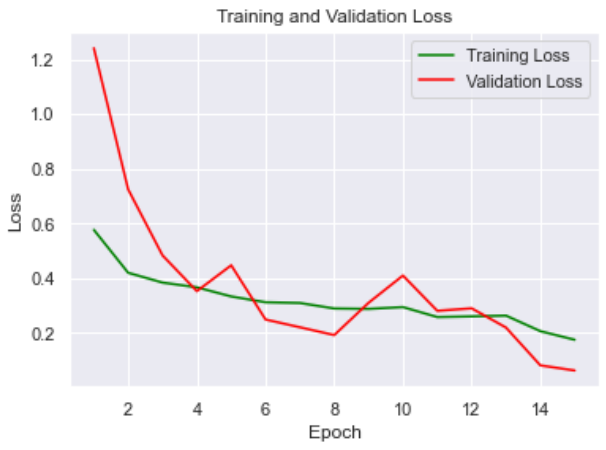

Figure 12. CNN-LSTM Loss on BT classification

The CNN-LSTM model is supplied with the test images to predict whether or not the image contains a tumor. The accuracy and loss achieved during the testing phase are 0.9567 and 0.1318, respectively, as illustrated in figure 13. According to the graph, the time required to anticipate the test images is 389ms.

```
25/25 [==============================] - 10s 389ms/step -
loss: 0.1318 - accuracy: 0.9567
```

Figure 13. CNN-LSTM outcome on test data

Both model CNN and CNN-LSTM are compared using the metrics like accuracy, loss, and time. And the comparison is given in Figure 14. The accuracy of CNN-LSTM is higher than the CNN at the rate of 0.0534. Next, the loss is evaluated. The loss and time value of CNN-LSTM is 0.1105 and 22ms lower than CNN. This comparison shows that the CNN-LSTM is better than the CNN in case of time and performance.

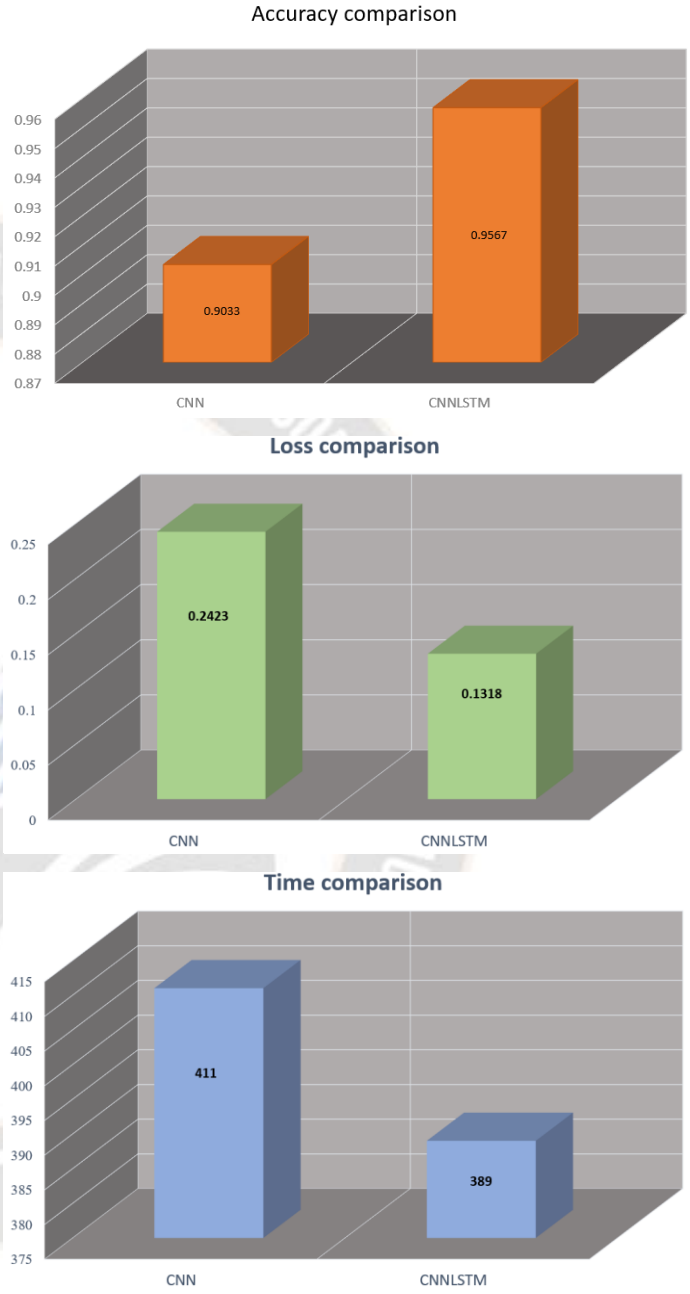

Figure 14. CNN and CNN-LSTM performance comparison

VII. CONCLUSION

Classification of BT is a crucial phase that calls for the expertise physician. To assist radiologists and clinicians in the identification of BT, an automated tumour categorization system is crucial. The research helps to identify the BT without the intervention of humans. To detect BT MRI data are collected from Kaggle. The data contains information like MRI samples with tumor masks and labels. This data will be helpful

International Journal on Recent and Innovation Trends in Computing and Communication
ISSN: 2321-8169 Volume: 11 Issue: 10s
DOI: https://doi.org/10.17762/ijritcc.v11i10s.7703
***Article Received:** 12 June 2023 **Revised:** 30 July 2023 **Accepted:** 10 August 2023*

for classification and segmentation. The data from Kaggle is first resized to a standard shape and then the pixel values are normalized in the range of 0 to 1. These two steps help to reduce computational power and time. Then the MRI is augmented using geometric techniques like rotation, flip, shear, etc and it will help make the system more robust. The U-Net is employed to segment the tumor from MRI. To do this the U-Net is trained using MRI and mask images. After training the U-Net model is evaluated using IoU and Dice coefficient. The IoU and Dice value attained by U-Net is 0.79445 and 0.8843. Then for classification DL models like CNN and CNN-LSTM are used. Both models are compared to identify the best one for tumor classification. For comparison accuracy and loss, metrics are used. From the comparison results, it is identified that the CNN-LSTM is identified to be the best.

For the future, the scope includes expanding the dataset with more diverse MRI data, incorporating transfer learning techniques, and integrating multiple imaging modalities for improved accuracy. Furthermore, efforts will be made to interpret the model's decisions, optimize for real-time application, conduct clinical validation studies, and extend the system to detect other organ abnormalities. These advancements will make the automated tumor categorization system more accurate, reliable, and applicable in clinical practice, leading to enhanced healthcare outcomes and early diagnosis of brain tumors.

REFERENCES

[1] Louis, David N., Arie Perry, Guido Reifenberger, Andreas Von Deimling, Dominique Figarella-Branger, Webster K. Cavenee, Hiroko Ohgaki, Otmar D. Wiestler, Paul Kleihues, and David W. Ellison. "The 2016 World Health Organization classification of tumors of the central nervous system: a summary." Acta neuropathologica 131 (2016): 803-820.

[2] Khan, Amjad Rehman, Siraj Khan, Majid Harouni, Rashid Abbasi, Sajid Iqbal, and Zahid Mehmood. "Brain tumor segmentation using K-means clustering and deep learning with synthetic data augmentation for classification." Microscopy Research and Technique 84, no. 7 (2021): 1389-1399.

[3] Logeswari, T., and M. Karnan. "An improved implementation of brain tumor detection using segmentation based on hierarchical self organizing map." International Journal of Computer Theory and Engineering 2, no. 4 (2010): 591.

[4] Wen, P., Land Zheng, and J. Zhou. "Spatial credibilistic clustering algorithm in noise image segmentation." In 2007 IEEE International Conference on Industrial Engineering and Engineering Management, pp. 543-547. IEEE, 2007.

[5] Habib, Hassan, Awais Mehmood, Tahira Nazir, Marrium Nawaz, Momina Masood, and Rabbia Mahum. "Brain Tumor Segmentation and Classification using Machine Learning." In 2021 International Conference on Applied and Engineering Mathematics (ICAEM), pp. 13-18. IEEE, 2021.

[6] Tazeen, Tasmiya, Mrinal Sarvagya, and M. Sarvagya. "Brain tumor segmentation and classification using multiple feature extraction and convolutional neural networks." International Journal of Engineering and Advanced Technology 10, no. 6 (2021): 23-27.

[7] Díaz-Pernas, Francisco Javier, Mario Martínez-Zarzuela, Míriam Antón-Rodríguez, and David González-Ortega. "A deep learning approach for brain tumor classification and segmentation using a multiscale convolutional neural network." In Healthcare, vol. 9, no. 2, p. 153. MDPI, 2021.

[8] Bal, Abhishek, Minakshi Banerjee, Punit Sharma, and Mausumi Maitra. "Brain tumor segmentation on MR image using K-Means and fuzzy-possibilistic clustering." In 2018 2nd international conference on electronics, materials engineering & nano-technology (IEMENTech), pp. 1-8. IEEE, 2018.

[9] Malathi, M., and P. Sinthia. "MRI brain tumour segmentation using hybrid clustering and classification by back propagation algorithm." Asian Pacific Journal of Cancer Prevention: APJCP 19, no. 11 (2018): 3257.

[10] Karayeğen, Gökay, and Mehmet Feyzi Akşahin. "Brain Tumor Prediction with Deep Learning and Tumor Volume Calculation." In 2021 Medical Technologies Congress (TIPTEKNO), pp. 1-4. IEEE, 2021.

[11] Asif, Sohaib, Wenhui Yi, Qurrat Ul Ain, Jin Hou, Tao Yi, and Jinhai Si. "Improving Effectiveness of Different Deep Transfer Learning-Based Models for Detecting Brain Tumors from MR Images." IEEE Access 10 (2022): 34716-34730.

[12] Raj, G. ., Verma, A. ., Dalal, P. ., Shukla, A. K. ., & Garg, P. . (2023). Performance Comparison of Several LPWAN Technologies for Energy Constrained IOT Network. International Journal of Intelligent Systems and Applications in Engineering, 11(1s), 150–158. Retrieved from https://ijisae.org/index.php/IJISAE/article/view/2487

[13] Ranjbarzadeh, Ramin, Nazanin Tataei Sarshar, Saeid Jafarzadeh Ghoushchi, Mohammad Saleh Esfahani, Mahboub Parhizkar, Yaghoub Pourasad, Shokofeh Anari, and Malika Bendechache. "MRFE-CNN: multi-route feature extraction model for breast tumor segmentation in Mammograms using a convolutional neural network." Annals of Operations Research (2022): 1-22.

[14] Baseri Saadi, Soroush, Nazanin Tataei Sarshar, Soroush Sadeghi, Ramin Ranjbarzadeh, Mersedeh Kooshki Forooshani, and Malika Bendechache. "Investigation of effectiveness of shuffled frog-leaping optimizer in training a convolution neural network." Journal of Healthcare Engineering 2022 (2022).

[15] Tataei Sarshar, Nazanin, Ramin Ranjbarzadeh, Saeid Jafarzadeh Ghoushchi, Gabriel Gomes de Oliveira, Shokofeh Anari, Mahboub Parhizkar, and Malika Bendechache. "Glioma Brain Tumor Segmentation in Four MRI Modalities Using a Convolutional Neural Network and Based on a Transfer Learning Method." In Proceedings of the 7th Brazilian Technology Symposium (BTSym'21) Emerging Trends in Human Smart and Sustainable Future of Cities (Volume 1), pp. 386-402. Cham: Springer International Publishing, 2022.

[16] Ms. Nora Zilam Runera. (2014). Performance Analysis On Knowledge Management System on Project Management. International Journal of New Practices in Management and

International Journal on Recent and Innovation Trends in Computing and Communication
ISSN: 2321-8169 Volume: 11 Issue: 10s
DOI: https://doi.org/10.17762/ijritcc.v11i10s.7703
***Article Received:** 12 June 2023 **Revised:** 30 July 2023 **Accepted:** 10 August 2023*

Engineering, 3(02), 08 - 13. Retrieved from http://ijnpme.org/index.php/IJNPME/article/view/28

[17] Ranjbarzadeh, Ramin, Abbas Bagherian Kasgari, Saeid Jafarzadeh Ghoushchi, Shokofeh Anari, Maryam Naseri, and Malika Bendechache. "Brain tumor segmentation based on deep learning and an attention mechanism using MRI multi-modalities brain images." Scientific Reports 11, no. 1 (2021): 1-17.

[18] Miller, J., Evans, A., Martinez, J., Perez, A., & Silva, D. Predictive Maintenance in Engineering Facilities: A Machine Learning Approach. Kuwait Journal of Machine Learning, 1(2). Retrieved from http://kuwaitjournals.com/index.php/kjml/article/view/113

[19] https://www.kaggle.com/datasets/mateuszbuda/lgg-mri-segmentation

[20] Danon, Dov, Moab Arar, Daniel Cohen-Or, and Ariel Shamir. "Image resizing by reconstruction from deep features." Computational Visual Media 7, no. 4 (2021): 453-466.

[21] Ding, Pengpeng, Jinguo Li, Liangliang Wang, Mi Wen, and Yuyao Guan. "HYBRID-CNN: An efficient scheme for abnormal flow detection in the SDN-Based Smart Grid." Security and communication networks 2020 (2020): 1-20.

[22] Mikołajczyk, Agnieszka, and Michał Grochowski. "Data augmentation for improving deep learning in image classification problem." In 2018 international interdisciplinary PhD workshop (IIPhDW), pp. 117-122. IEEE, 2018.

[23] Shorten, Connor, and Taghi M. Khoshgoftaar. "A survey on image data augmentation for deep learning." Journal of big data 6, no. 1 (2019): 1-48.

[24] Li, Lin, Peeter Ross, Maarja Kruusmaa, and Xiaosong Zheng. "A comparative study of ultrasound image segmentation algorithms for segmenting kidney tumors." In Proceedings of the 4th international symposium on applied sciences in biomedical and communication technologies, pp. 1-5. 2011.

[25] Siddique, Nahian, Sidike Paheding, Colin P. Elkin, and Vijay Devabhaktuni. "U-net and its variants for medical image segmentation: A review of theory and applications." IEEE Access 9 (2021): 82031-82057.

[26] Yin, Xiao-Xia, Le Sun, Yuhan Fu, Ruiliang Lu, and Yanchun Zhang. "U-Net-Based medical image segmentation." Journal of Healthcare Engineering (2022).

[27] Faris, W. F. . (2020). Cataract Eye Detection Using Deep Learning Based Feature Extraction with Classification. Research Journal of Computer Systems and Engineering, 1(2), 20:25. Retrieved from https://technicaljournals.org/RJCSE/index.php/journal/article/view/7

[28] Ronneberger, Olaf, Philipp Fischer, and Thomas Brox. "U-net: Convolutional networks for biomedical image segmentation." In Medical Image Computing and Computer-Assisted Intervention–MICCAI 2015: 18th International Conference, Munich, Germany, October 5-9, 2015, Proceedings, Part III 18, pp. 234-241. Springer International Publishing, 2015.

[29] Liu, Tianyi, Shuangsang Fang, Yuehui Zhao, Peng Wang, and Jun Zhang. "Implementation of training convolutional neural networks." arXiv preprint arXiv:1506.01195 (2015).

[30] Rashid, Junaid, Saba Batool, Jungeun Kim, Muhammad Wasif Nisar, Amir Hussain, Sapna Juneja, and Riti Kushwaha. "An augmented artificial intelligence approach for chronic diseases prediction." Frontiers in Public Health 10 (2022).

[31] Ayadi, Wadhah, Wajdi Elhamzi, Imen Charfi, and Mohamed Atri. "Deep CNN for brain tumor classification." Neural Processing Letters 53 (2021): 671-700.

[32] Luan, Yuandong, and Shaofu Lin. "Research on text classification based on CNN and LSTM." In 2019 IEEE international conference on artificial intelligence and computer applications (ICAICA), pp. 352-355. IEEE, 2019.

[33] Chen, Gang. "A gentle tutorial of recurrent neural network with error backpropagation." arXiv preprint arXiv:1610.02583 (2016).

[34] Hochreiter, Sepp. "The vanishing gradient problem during learning recurrent neural nets and problem solutions." International Journal of Uncertainty, Fuzziness and Knowledge-Based Systems 6, no. 02 (1998): 107-116.